SolarPACES 2024, 30th International Conference on Concentrating Solar Power, Thermal, and Chemical Energy Systems

Thermal Energy Storage Materials, Media, and Systems

https://doi.org/10.52825/solarpaces.v3i.2464

Published: 25 Nov. 2025

Numerical Analysis on the State of Charge of an Ultra-High Temperature Latent Heat Thermal Energy Storage System

The Case Study of FeSiB Alloy Phase Change

Myrto Zeneli[1,*] and Alejandro Datas[1]

[1]Instituto de Energía Solar, Madrid, Spain

*Correspondence: Myrto Zeneli, m.zeneli@upm.es

Abstract. Ultra-high temperature thermal energy storage (UHTES) and conversion is an emerging field of technology that enables much higher energy densities (>1 MW_{th}) and conversion efficiencies than conventional thermal energy storage technologies. Our research group of Solar Energy Institute is currently developing a novel latent heat thermophotovoltaic (LHTPV) battery that utilizes Si-based alloys to store either surplus renewable electricity or concentrated sunlight in the form of latent heat at temperatures close to 1200 ºC and convert it back to electricity on demand. Determining the State of Charge (SoC) of this ultra-high temperature thermal battery is imperative to regulate its real-time operation and optimize its performance. However, using of several sensors within the storage system –as mainly done in low temperature phase change materials (PCMs) to quantify their SoC - becomes costly and challenging for this range of operating conditions. This study presents a numerical method, which is used to get an understanding of the physical processes taking place during the LHTPV operation and capture comprehensive data of time varying flow variables that can be difficult to record during real-time operation. Our results indicate that we can describe the system's SoC by measuring the time-varying temperature at its sidewalls and the input/output heat flux values, without the need of knowing beforehand the thermophysical properties of the used materials. Based on these variables we can define several indicators that can help us obtain a better understanding of the required physical signals to be measured in order to determine its SoC, during real-time operation.

Keywords: State of Charge, Thermal Energy Storage, Numerical Simulation

1. Introduction

The urgent need for decarbonization necessitates a global switch towards low emission fuels or clean energy alternatives. The most potent decarbonization strategy is increasing the share of Renewable Energy Sources (RES) in the energy mix. Thermal energy storage (TES) is a game changer technology, essential for optimizing the use of the intermittent RES, owing to its ability of storing the excess electricity from variable RES (solar and wind) or directly storing of solar energy in the form of heat, which can be converted into electricity on demand. Ultra-high temperature thermal energy storage (UHTES) is an emerging field of science and technology [1] that enables much higher energy densities (>1 MWh_{th}) and heat-to-electricity conversion efficiencies than conventional TES technologies, i.e. molten salts, which operate at

maximum temperatures of ~600 ºC. Among the several UHTES solutions that are being developed, UPM is developing at its premises in Madrid a pilot-scale thermal battery [2] that stores either surplus renewable electricity (power-to-heat-to-power-P2H2P) or concentrated sunlight (solar-to-heat-to-power-S2H2P) in the form of latent heat at extreme temperatures (over 1200 ºC) and converts it back to electricity on demand by using advanced thermophotovoltaic technology. This Latent Heat Thermophotovoltaic (LHTPV) battery (Figure 1) is a compact (10 times higher than concentrated solar power - CSP) device that can store thermal energy at low costs (< 10 €/kWh$_{th}$). The technology uses silicon-based phase change materials (PCMs) for TES and thermophotovoltaic (TPV) generators for thermal-to-electric energy conversion. TPV devices have similar operation to solar cells, but they are converting thermal radiation, instead of sunlight, into electricity. TPVs consist of an incandescent emitter (temperatures > 1000 ºC) that radiates photons towards TPV cells, which produce electricity through the photovoltaic effect. This device has reached 40 % conversion efficiencies [3, 4], being as efficient as commercial steam turbines. The high efficiency combined with a simple and compact design (e.g. lack of heat transfer fluids or moving parts) open the road for a new type of technology that can lead in the solar energy field during the forthcoming decades.

A fundamental challenge in this breakthrough concept is defining its state-of-charge (SoC), when operating in a cycling performance. Monitoring the SoC is necessary for the optimal, efficient and safe operation of a TES system, which can become challenging when operating at ultra-high temperatures. In latent heat thermal energy storage units, this can be equivalent with the amount of the stored latent heat or the liquid fraction (LFR: ratio of liquid PCM to overall PCM mass) values [5]. A possible approach to define such parameters is to utilize several probes to measure the temperature change across the PCM volume or at the crucible sidewalls, whereas additional data such as the PCM thermal properties are usually required, even for data-driven approaches currently available in the recent literature [6]. In a practical application, quantifying accurately the PCM thermal properties becomes often challenging. Thus, there is a need for defining the SoC of a LHTES system by relying only on operating parameters, such as input/output heat flux and temperature values.

The present work studies a LHTES system, which will be operating with measuring probes on the exterior surfaces of the crucible, due to the demanding operating conditions. A numerical model is developed to observe the transient response of the system under both charging and discharging phases and gain a better understanding on the specific requirements that need to be met to install the necessary equipment in a real time operation. This model has the capacity of simulating the melting (charging) and solidification (discharging) process of the battery and to capture comprehensive data on time varying flow variables (both local and global) that can be difficult and expensive to record during real-time operation, owing to the corresponding sophisticated instrumentation required. Several indicators are quantified in order to assist the measuring process. Such analysis aims for the first time to extract generalized results for a thermal energy storage system´s behavior and SoC, by relying only on real-time measured operating parameters (temperature and heat flux), decoupling, thus, the SoC definition by the material thermal properties already used in previous works.

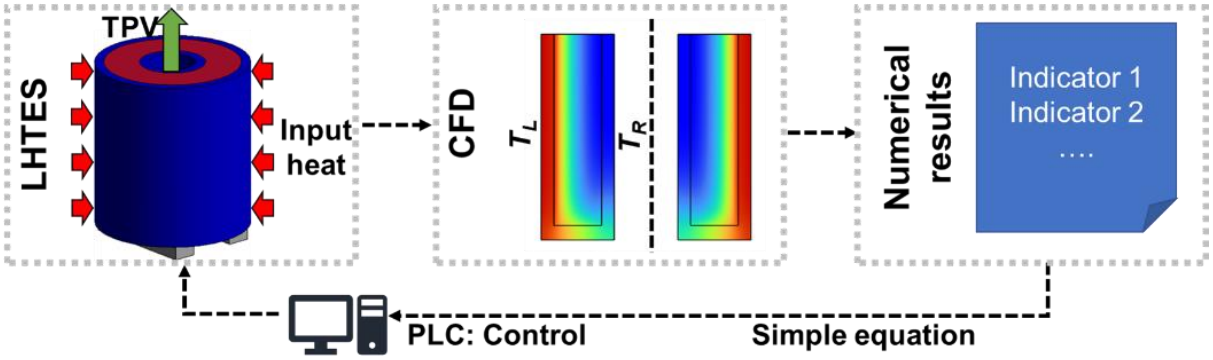

***Figure 1**. Schematic of the LHTPV battery system numerical strategy to define its SoC (T_L: Outer wall temperature, T_R: Inner wall temperature facing the TPV converter).*

2. Numerical model

A transient computational fluid dynamics (CFD) model based on the enthalpy-porosity approach [7], available in Ansys Fluent™ (v24.R2) platform is used for the simulations. The CFD model applied in this work has been previously verified against an analytical model [8], describing the silicon solidification process inside a sealed crucible and validated against experimental measurements [9] for paraffin wax melting at low temperatures, owing to the lack of experimental data for such high temperatures. Some of the assumptions adopted include:

1. Transient fluid flow and heat transfer mechanisms;
2. Inclusion of gravity effect;
3. Solution of laminar flow conditions, due to low Reynolds numbers for the cases studied;
4. The molten PCM is treated as an incompressible Newtonian fluid;
5. Both solid and liquid phases of the PCM are homogeneous and isotropic;
6. Temperature dependent thermophysical properties of the PCM and crucible;
7. The PCM density is constant;
8. Radiative heat transfer within the vessel is neglected;
9. Contact thermal resistances between solid/liquid PCM and walls are negligible;
10. Evaporation of any contained gas (probably observed during the initial cycles of the phenomenon) is not considered.

A more detailed analysis of the enthalpy porosity equations can be found in [8] and [10]. Concerning the SoC definition, we use a liquid fraction-based approach according to which:

$$\mathrm{SoC} = \mathrm{LFR(t)} \tag{1}$$

The main parameters that can be used to implicitly quantify its LFR and, thus, and its SoC include the a) Time-varying area weighted average temperature at the battery sidewalls (T) b) Input / Output flux (constant Q or time variable Q(t)), and c) charging/discharging time (t).

2.1 Geometry and mesh

The physical domain is a cylindrical crucible made of graphite inside which a FeSiB alloy undergoes solidification-melting through a cycling performance (Figure 1). Both the PCM and the crucible are explicitly simulated as fluid and solid domains, respectively. Owing to the crucible's symmetry across the central axis a 2D axisymmetric case is simulated to reduce the induced computational cost. Furthermore, a conformal grid of 6,348 quadrilateral elements is utilized to increase the level of accuracy, near the phase-change region. This grid has been chosen based on a preliminary grid independence study comparing 3 grids of a) 6,348, b) 25,392 and 50,784, results of which can be found in the Supplementary material.

2.2 Model set-up

Concerning the model set-up, the most important parameter in the enthalpy-porosity approach, which affects the PCM melting rate, is the mushy zone parameter. This parameter is usually taken by default equal to 10^5. Based on the previous experience of the authors regarding the solidification-melting of Si alloys this parameter can be quantified as follows [11]:

$$\mathrm{A_{mush}} = 180\frac{\mu}{\rho\, SDAS^2} \tag{2}$$

, where μ is the liquid PCM viscosity, ρ is its density and SDAS the secondary dendrites arm spacing. By assuming an indicative SDAS value of 40 μm for FeSiB alloys we get an A_{mush} value of $5*10^5$. It should be noted that in order to accurately predict the melting behavior of a specific PCM an experimentally measured value of the SDAS should be used. In the solidification process, which is a conduction dominated process this parameter does not affect significantly the phase-change rate. Indicative materials properties can be found in [12].

2.3 Boundary and operating conditions

Appropriate boundary conditions are set at the crucible sidewalls. During charging phase (melting), a constant input heat flux flows into the domain through the crucible (outer) wall. During discharging phase (solidification), a constant heat flux is extracted from the TPV converter, which faces the crucible inner wall. Adiabatic conditions are assumed for the upper and bottom crucible walls. At initial conditions, the whole domain is patched to 27 ºC (melting phase). The solidification process starts right after the PCM melting ends.

Three states are used during melting phase (I. sensible heat storage: only solid phase, II. latent heat and sensible heat storage: phase change, III. sensible heat storage: only liquid phase). The same applies for the solidification phase (IV. sensible heat extraction: only liquid phase, V. latent heat and sensible heat extraction, VI. sensible heat extraction: only solid phase). During calculation, the transient response of the wall temperature is monitored for heat flux values within $[5Q_{ref} - Q_{ref}/5]$, with Q_{ref} = 143 kW (it is the energy required for phase-change of 1-2 h) and several indicators are derived to describe the system's SoC, indicatively described for charging phase. The overall PCM mass is equal to 717 kg, whereas the volume is equal to 0.134 m^3 of the PCM itself and 0.221 m^3 of the whole system.

3. Results and discussion

3.1 SoC indicators

3.1.1 1st indicator: Time-varying wall temperature

This a common indicator used to describe a system's SoC. Figure 2 shows that the outer wall temperature (T_L) follows a linear profile during the PCM preheating (only solid) and then undergoes a slope change, when the PCM melting starts (point 1). This steep change signifies the quick transition from solid to liquid phase at this area. As the phenomenon evolves, the phase-change front moves inwards the domain until it reaches the crucible inner surface (touching the TPV) and the temperature there (T_R) changes accordingly (point 2). From this point and onwards the T_R is almost constant owing to the phase change phenomenon evolution at the inner surface. When the solidification-melting ends, the temperature at this surface increases abruptly (point 3). Although being rather simple to monitor, it is evident that due to the system's complex dynamics during real-time application it is difficult to understand the meaning of such temperature changes, especially when they are not steep, and, thus, extract accurately the system's SoC.

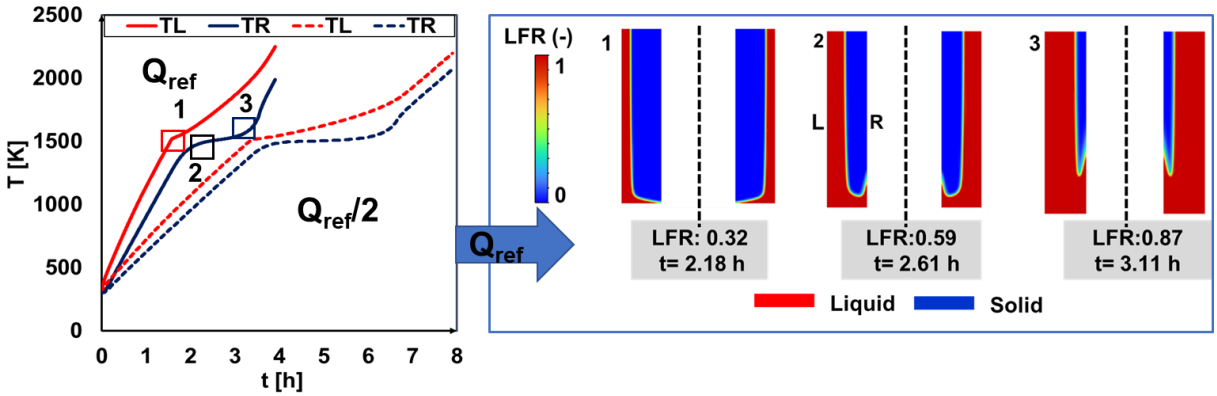

***Figure 2**. Time variation of the wall temperature values of the LHTPV battery (melting, Q_{ref} -, $Q_{ref}/2$ --).*

3.1.2 2nd indicator: Time varying D(T_L-T_R)/dt rate

A more accurate representation of the system SoC arises from the time evolution of the global temperature gradient (DT/dt) rate with time. Notably, in this case the temperature is monitored not as an absolute value at each surface of interest. On the contrary, the temperature difference between the two surfaces is monitored, i.e. T = T_L-T_R is used to describe this variable. Based on the numerical analysis valuable results can be extracted for the DT/dt: D(T_L-T_R)/dt response during both the charging and discharging phases (Figure 3a-c).

During charging (Figure 3a), the PCM starts from the sensible phase (state I). In this region, the DT/dt gradient starts at a high value during the system start-up and declines until it reaches a small value (in the order of ~1. e-3 K/s for Q equal to Q_{ref}). During this state, the system behaves as a conductive material and the incoming heat is stored into the system in the form of sensible heat. When the phase-change state starts (state II) an abrupt change in the DT/dt gradient is observed. During this state, the DT/dt gradient tends to increase – signifying a deceleration mechanism on the system temperature increase- owing to the high latent heat source term, required for the phase change. When the melting phenomenon finishes, the DT/dt gradient undergoes a rapid change and then the DT/dt value tends to stabilize in a small value, likewise to state I. A similar phenomenon is observed in the PCM discharging phase, Figure 3b.

It should be noted that the lower the heat flux input/output the lower the change of magnitude of the DT/dt variable during the transition from the different States. On the other hand, as Q increases, significant oscillations of the DT/dt variable are observed, during the initial minutes of the phase change process (e.g. yellow line in Figure 3c), making it difficult to define the starting point of the phase change process.

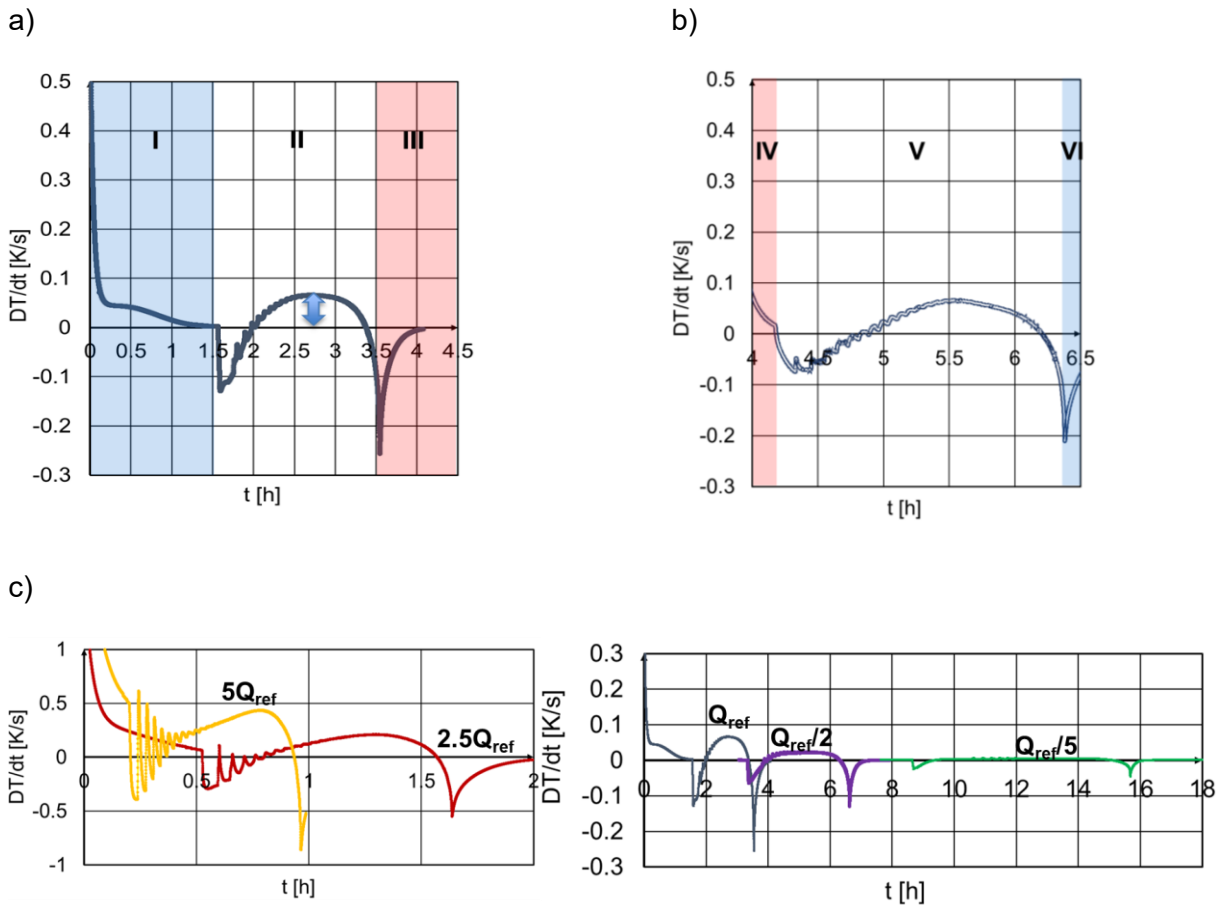

***Figure 3**. Time variation of the area-weighted average temperature difference (TL-TR) gradient rate with time during a) melting and b) solidification phase for Qref, and, c) melting phase for all cases (blue region: solid state, pink region: liquid state, white region: phase-transition state).*

3.1.3 3rd indicator: (DT/dt/Q) variation with PCM melt fraction (LFR)

In real time application, the Q value (influx/outflux) will be time-varying. Thus, it is important to observe the phase-change behavior of the system for different Q values. As can be noticed, almost similar profiles are achieved of the (DT/dt)/Q variation with the LFR values, Figure 4a. This is an important observation, for the description of the phase-changing process as it leads to the conclusion that a general equation combining these two parameters can be extrapolated based on the numerical results. Such an equation – or a similar one - can be incorporated into the PLC algorithm to describe the SoC of the system based on only experimentally measured parameters (a) the temperature at the walls, T and b) the input/output heat flux, Q).

Another conclusion drawn is that the PCM liquid fraction follows an almost linear profile, Figure 4b, during the phenomenon evolution, for the specific range of operating conditions studied. Thus, by knowing the starting and ending point of the PCM phase we can estimate the LFR by a linear interpolation (assuming the heat input/output) is constant for a specific time interval. This can be extracted by observing the changing in the DT/dt gradient with time, Figure 3. For this process, historical data are needed during the system real-time operation.

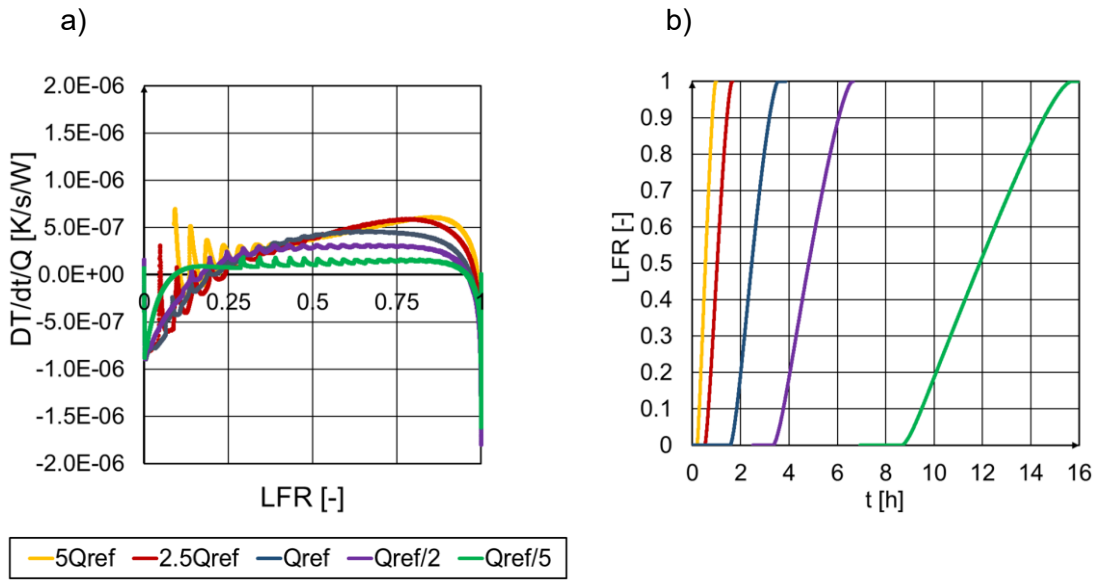

Figure 4. *a) (DT/dt/Q) gradient with LFR (LFR: 0 = solid, 1 = liquid) and b) time variation of the PCM liquid fraction for several Q_{in} values (melting phase).*

3.1.4 4th indicator: Temperature uniformity

A supplementary indicator is the temperature uniformity index, UI (a dimensionless number varying within 0 and 1, where 0 indicates poor uniformity and 1 indicates perfect uniformity [13]) at the crucible sidewalls. While this parameter does not explicitly describe the SoC of the system, it is crucial to quantify it numerically to determine the number and placement of the measurement probes to be used during the experimental campaigns. During the charging phase (Figure 5a) as the phase change progresses, the solid-liquid front reaches the inner surface of the crucible (close to the TPV), thereby affecting the temperature field. Owing to a non-uniform phase-changing front in this surface (Figure 2) and, thus, a non-uniform heat transfer mechanism (partly in the form of sensible heat and partly as latent heat), a non-uniform temperature profile is created in this region. On the contrary, at the outer surface (heated wall) the liquid fully PCM occupies the surface from the start of the phase change, resulting in a high temperature uniformity (with the uniformity index close to unity).

During the discharging phase (Figure 5b) the reverse occurs. The solid phase forms uniformly at the inner surface of the crucible first. Then, the phase-changing front moves gradually towards the outer crucible surface. In the final stages of the phase change, a slight inhomogeneity in the temperature distribution is observed at the outer crucible walls, owing to the non-homogeneous phase-changing front formed at this area. To obtain accurate temperature measurements, multiple probes are required, given the non-uniform temperature profiles during both processes. The higher the heating and/or cooling rate the greater the number of probes needed to properly capture the phenomenon. Notably, for heating/cooling rates exceeding Q_{ref} the minimum uniformity index drops below 0.95 during the phase change process.

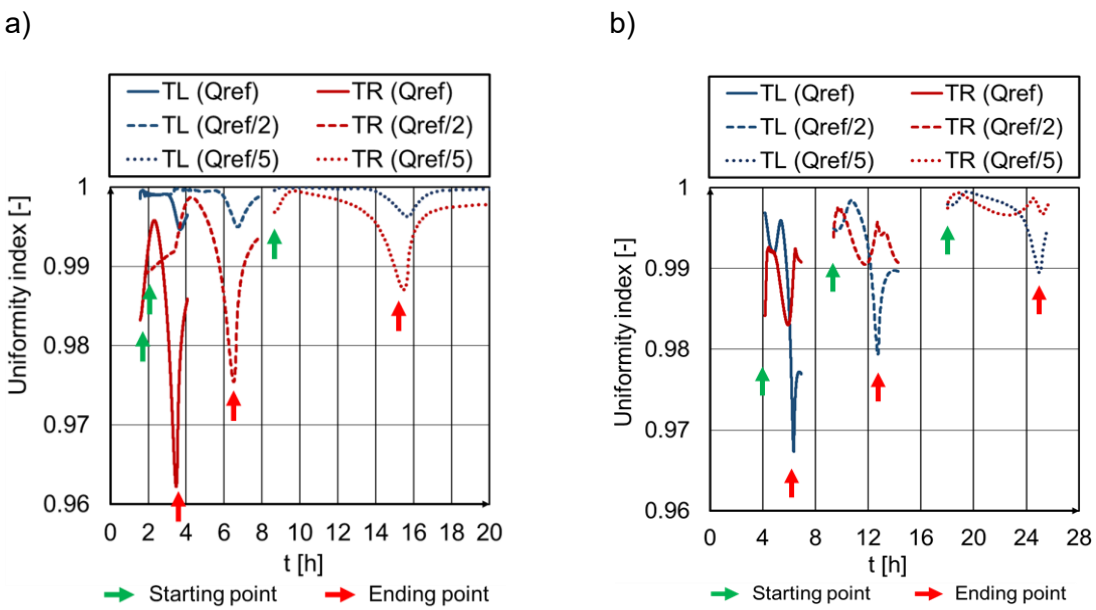

***Figure 5**. UI vs. time for Q_{ref}, $Q_{ref}/2$ and 2.5 $Q_{ref}/5$ (a: melting and b: solidification phase).*

4. Conclusions

In this work, we introduce a theoretical analysis for evaluating the state of charge (SoC) of a latent heat thermophotovoltaic battery operating at ultra-high temperatures (~1200 ºC). We utilize an advanced transient computational fluid dynamics model to introduce and quantify several indicators that allow for the estimation of the SoC using only the external wall temperature of the PCM container and the input/output heat flux data. The numerical results demonstrate that monitoring these operating parameters is sufficient for accurately tracking the SoC, a finding that holds potential for applications where sensor placement within the PCM is challenging, as in ultra-high temperature applications. Furthermore, this approach demonstrates that there is no need to know a priori the system's thermophysical properties, simplifying the SoC estimation during its real-time operation. In a future analysis, our research group envisages to develop a generic model capable of defining the SoC for a wide range of operating conditions, PCMs, and crucible dimensions by using a data-driven analysis. This model can be, then, incorporated into a PLC to monitor during real-time operation the system´s SoC. Concluding, the analysis provides initial conclusions for a specific PCM and operating conditions, paving the way for a more generic model to be developed in future studies.

Author contributions

Myrto Zeneli: Writing original draft, Methodology, Formal Analysis, Data Curation, Visualization; **Alejandro Datas**: Writing – review & editing, Methodology, Supervision

Data availability statement

Data supporting the results of the article can be accessed through excel files in Zenodo repository (https://doi.org/10.5281/zenodo.13758813).

Underlying and related material

Simulation results are deposited on Zenodo repository (//doi.org/10.5281/zenodo.13758813)

Competing interests

"The authors declare that they have no competing interests."

Funding

This project has received funding from the European Union's Horizon 2020 research and innovation programme under the Marie Skłodowska-Curie grant agreement SHINE (GA:101145914). Part of the work has been also carried out within THERMOBAT project under grant agreement 101057954. Views and opinions expressed are however those of the authors only and do not necessarily reflect those of the European Union. Neither the European Union nor the granting authority can be held responsible for them.

References

[1] A. Datas, "Preface," in Ultra-High Temperature Thermal Energy Storage, Transfer and Conversion, A. Datas, Ed., ed: Woodhead Publishing, 2021, pp. xi-xii.
[2] A. Datas, A. López-Ceballos, E. López, A. Ramos, and C. del Cañizo, "Latent heat thermophotovoltaic batteries," Joule, vol. 6, pp. 418-443, 2022/02/16/ 2022.
[3] A. LaPotin, K. L. Schulte, M. A. Steiner, K. Buznitsky, C. C. Kelsall, D. J. Friedman, et al., "Thermophotovoltaic efficiency of 40%," Nature, vol. 604, pp. 287-291, 2022/04/01 2022.
[4] B. Roy-Layinde, J. Lim, C. Arneson, S. R. Forrest, and A. Lenert, "High-efficiency air-bridge thermophotovoltaic cells," Joule, vol. 8, pp. 2135-2145, 2024/07/17/ 2024.
[5] W. Beyne, K. Couvreur, I. T'Jollyn, S. Lecompte, and M. De Paepe, "Estimating the state of charge in a latent thermal energy storage heat exchanger based on inlet/outlet and surface measurements," Applied Thermal Engineering, vol. 201, p. 117806, 2022/01/25/ 2022.
[6] H. Bastida, I. De la Cruz-Loredo, P. Saikia, and C. E. Ugalde-Loo, "Discrete-time state-of-charge estimator for latent heat thermal energy storage units based on a recurrent neural network," Applied Energy, vol. 371, p. 123526, 2024/10/01/ 2024.
[7] A. D. Brent, V. R. Voller, and K. J. Reid, "Enthalpy-porosity technique for modelling convection-diffusion phase change: Application to the melting of a pure metal," Numerical Heat Transfer, vol. 13, pp. 297-318, 1988/04/01 1988.
[8] A. Datas, M. Zeneli, C. del Cañizo, I. Malgarinos, A. Nikolopoulos, N. Nikolopoulos, et al., "Molten silicon storage of concentrated solar power with integrated thermophotovoltaic energy conversion," AIP Conference Proceedings, vol. 2033, p. 090005, 2018/11/08 2018.
[9] M. Zeneli, I. Malgarinos, A. Nikolopoulos, N. Nikolopoulos, P. Grammelis, S. Karellas, et al., "Numerical simulation of a silicon-based latent heat thermal energy storage system operating at ultra-high temperatures," Applied Energy, vol. 242, pp. 837-853, 2019/05/15/ 2019.
[10] E. Assis, L. Katsman, G. Ziskind, and R. Letan, "Numerical and experimental study of melting in a spherical shell," International Journal of Heat and Mass Transfer, vol. 50, pp. 1790-1804, 2007/05/01/ 2007.
[11] S. Minakawa, I. V. Samarasekera, and F. Weinberg, "Centerline porosity in plate castings," Metallurgical Transactions B, vol. 16, pp. 823-829, 1985.
[12] J. Jiao, Bettina Grorud, Caroline Sindland, Jafar Safarian, Kai Tang, Kathrine Sellevoll, and Merete Tangstad, "The Use of Eutectic Fe-Si-B Alloy as a Phase Change Material in Thermal Energy Storage Systems," Materials, vol. 12, 2019.
[13] "ANSYS fluent 24.R2 Theory Guide," 2024.